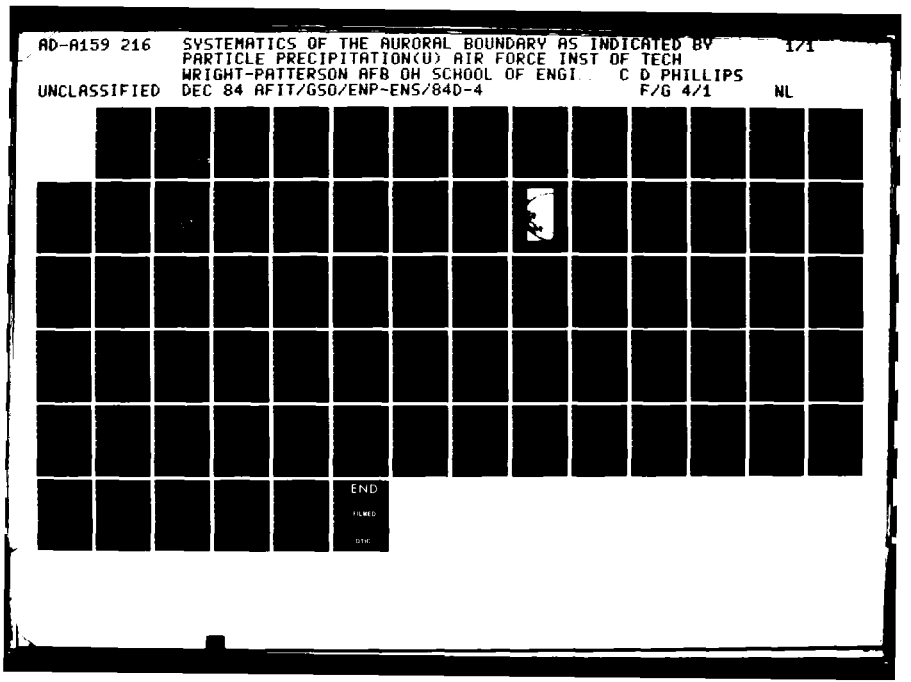
AD-A159 216
SYSTEMATICS OF THE AURORAL BOUNDARY AS INDICATED BY
PARTICLE PRECIPITATION(U) AIR FORCE INST OF TECH
WRIGHT-PATTERSON AFB OH SCHOOL OF ENGI
C D PHILLIPS
1/1
UNCLASSIFIED
DEC 84 AFIT/GSO/ENP-ENS/84D-4
F/G 4/1
NL
END
FILMED
DTIC

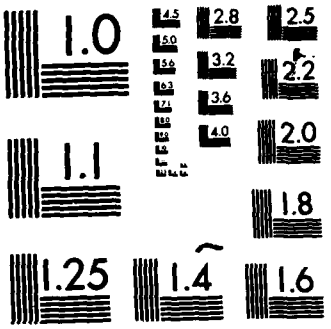

MICROCOPY RESOLUTION TEST CHART
NATIONAL BUREAU OF STANDARDS-1963-A

BOUNDARY AS INDICATED BY PARTICLE PRECIPITATION

THESIS

Charles D. Phillips
Captain, USAF

AFIT/GSO/ENP-ENS/84D-4

DEPARTMENT OF THE AIR FORCE
AIR UNIVERSITY
AIR FORCE INSTITUTE OF TECHNOLOGY

Wright-Patterson Air Force Base, Ohio

AFIT/GSO/ENP-ENS/84D-4

SYSTEMATICS OF THE AURORAL BOUNDARY AS INDICATED BY PARTICLE PRECIPITATION

THESIS

Charles D. Phillips
Captain, USAF

AFIT/GSO/ENP-ENS/84D-4

Approved for public release; distribution unlimited

AFIT/GSO/ENP-ENS/84D-4

SYSTEMATICS OF THE AURORAL BOUNDARY AS INDICATED BY PARTICLE PRECIPITATION

THESIS

Presented to the Faculty of the School of Engineering

of the Air Force Institute of Technology

Air University

In Partial Fulfillment of the

Requirements for the Degree of

Master of Science in Space Operations

Charles D. Phillips, B.S.

Captain, USAF

December 1984

Preface

This thesis closes out a very exciting time for me. It has certainly been a privilege (and a humbling experience) to have worked with the caliber of people that I worked with on this thesis. Fortunately, I was able to find a topic that was so interesting, and I hope that I have made some small contribution to the understanding of the aurora. It was very rewarding for me to be able to work on a problem of interest to the Air Force Geophysics Laboratory, and I am sure that they will enjoy continued success in their efforts. I hope that the cooperation between AFIT and the Laboratory will be continued in the coming years.

Several people have been invaluable during the course of this effort. Foremost among them was Maj James Lange. Without his guidance and encouragement this thesis would have been nearly impossible. Ms Nancy Heinemann of Boston College gave a lot of time and effort to get me started on the project and guide me through to finish it. Drs Susan Gussenhoven and David Hardy contributed their knowledge, and were patient with a newcomer to the field. I would like to thank the administration at AFGL who gave Drs Gussenhoven and Hardy the freedom to spend time with a student from a far off school. Thanks also are due to Lt Col Joseph Coleman, my other co-advisor, for his help with the statistics in this study.

Table Of Contents

Page

Preface.....ii

List Of Figures.....v

List Of Tables.....vi

Abstract.....vii

I. Introduction.....1

- Problem Statement.....2
- Objective Of The Research.....3
- Scope.....3

II. Background.....4

- Sources Of Magnetospheric Particles.....4
- Magnetospheric Particle Motion.....6
- The Near-Earth Magnetosphere.....7

III. Literature Review.....14

IV. Data Source And Preparation.....17

- Satellite Orbit.....17
- Instrument.....18
- Calibration.....19
- Boundary Selection.....25
- Data Sources.....29

V. Methodology.....31

- Linear Regression.....31
- Data Subdivisions.....33
- The General Linear Test.....35
- Processing Equipment And Software.....37

VI. Results.....38

- Analysis Of Auroral Boundary Behavior.....38
- Relationship Of Electron And Ion Boundaries.....47

VII. Conclusions And Recommendations.....55

- Conclusions.....55
- Recommendations.....56

Bibliography.....BIB - 1

Vita.....V - 1

List Of Figures

Figure Page

1. The Earth's Magnetosphere.....5
2. The Aurora.....11
3. DMSP/F7 Orbital Coverage.....18
4. Electron/Ion Spectrometer (SSJ/4).....20
5. Format Of F7 Flux Plot.....26
6. Computed Electron/Ion Boundary Differences.....50
7. Plotted Linear Regression λ_0s (Polar).....51
8. Plotted Linear Regression λ_0s (Mercator).....52

List Of Tables

Table Page

1. Results Of Linear Regression On Initial Boundary Grouping.....39
2. Linear Regression Results On Separated Hour Bins..41
3. Comparison Of Regression Line Slopes.....43
4. Linear Regression Results On Combined Pole Hour Bins.....44
5. Comparison Of Combined And Separated Hour Bins....45
6. Regression Line Equivalence Test Results.....46
7. Mean Computed Auroral Boundary Differences.....48
8. Computed Mean Difference In Separated Hour Bins...49

Abstract

This thesis examined several ways of grouping data acquired by the DMSP/F7 satellite's electron and ion spectrometers, and used that data to decide the relationship between the latitude of the equatorward boundary of the electron and ion diffuse aurora. The statistical analysis was done with the SPSS computer package and data from the Special Sensor J/4 on board the Defense Meteorological Satellite Program F7 (Block 5D) spacecraft. The analytic technique used was bivariate linear regression, with the General Linear Test for the equality of two regression lines being used to compare different regression lines.

This analysis of precipitating electrons and ions above the polar regions at about 840 kilometers found that the precipitation at different geomagnetic longitudes can be accurately represented by dividing the measured boundaries according to their magnetic local times of occurrence. Three hour wide bins were attempted, and were found to be less desirable than one hour wide bins. It was found that measured boundaries from the two poles can be combined in a single regression line.

The above results were used to find that the equatorward boundary of the diffuse ion aurora is circular and poleward of the equatorward boundary of the diffuse electron aurora, except for a few hours in the midnight sector. This study

finds that one of the points where the ion aurora and electron aurora cross is in the 2100 hour bin.

SYSTEMATICS OF THE AURORAL BOUNDARY AS INDICATED BY PARTICLE PRECIPITATION

I. Introduction

Since the discovery of the Van Allen radiation belts in 1958, scientists realized that the region just beyond the Earth's atmosphere had considerable structure and complexity. Extensive studies of the aurora were done from the ground, and ground-based observations still are central in the studies of the aurora. Among the devices used to observe the aurora from the ground are all-sky cameras, radars, and various electric and magnetic field measurement instruments. These devices are limited to the study of the interaction of the magnetosphere and the atmosphere rather than measuring the magnetosphere itself. Since the advent of orbiting satellites and space probes, numerous platforms for the study of the magnetosphere have become available. Some of them range well beyond the limits of the magnetosphere, both towards and away from the Sun. From platforms such as these, one can observe interplanetary space, free from the effects of the Earth. Some of the monitoring platforms are in high orbits around the Earth - such as geosynchronous orbits. From them, the Earth's magnetic field can be directly measured. Some observations can be made from orbits close to the Earth. These observations can measure the magnetic field's structure

close to the top of the atmosphere. One of the very near Earth indicators of the state of the magnetosphere involves the auroral zone. Many features of the aurora can be shown to have sources deep in the magnetosphere.

Researchers at the Air Force Geophysics Laboratory (AFGL), Hanscom AFB, Massachusetts, have been examining the equatorward boundary of the auroral zones for several years. One of the sources of their data has been the Defense Meteorological Satellite Program (DMSP) operational satellites. Beginning with the F2 satellite in July of 1977, they have had particle spectrometers mounted on them to detect auroral particles. The early satellites had only electron spectrometers, and using that data they developed ways to determine the limits of auroral precipitation and a model for the behavior of this auroral boundary with changes in the Earth's magnetic field. Beginning with the F6 satellite in December of 1982, the satellites have carried both electron and ion spectrometers. This supplies a new data population to which the earlier analyses can be extended. In addition, there are several ways of grouping the available data, and several popular indices of the Earth's magnetic field strength.

Problem Statement

An analysis will be done to compare different ways of grouping the measured auroral boundaries when correlating them with the geomagnetic activity index Kp. The use of the

real time ap index as provided by the Air Force Global Weather Central (AFGWC) will be investigated. Finally, the analyzed data should be used, together with data from an earlier study by AFGL, to determine the separation of the equatorward boundaries of diffuse electron and ion aurora.

Objective of the Research

This thesis will apply statistical procedures to compare different methods of grouping measured auroral boundaries, and use the chosen method to extend the model for the separation of the electron and ion aurora. By comparing the different ways of grouping the measured boundaries, one can infer what drives the precipitation of particles from deeper in the magnetosphere. Knowledge of the differences in behavior of the electron and ion precipitation also will shed light on the forces at work in the magnetosphere.

Scope

This study of particle precipitation is limited to electrons and ion with energies between 30 eV and 30 keV, as observed by the DMSP/F7. The data for this study covers the first three weeks of December 1983. F7 results in this study will be combined with previously reported results (Hardy, 1984a) from F6 for furthur analysis.

II Background

Sources Of Magnetospheric Particles

The aurora is one of the products of the expansion of the solar atmosphere. This expansion is the source of the solar wind - a thin gas of charged particles which "blows" radially away from the Sun. As it expands, the solar magnetic field orientation is "frozen" into pockets of gas. (Lange, 1983:III-A-4) When this gas encounters the magnetic field of the Earth, a complex interaction begins. The Earth's magnetic field is compressed until the pressure generated by it's field strength equals that of the Solar wind flow motion. (Lange, 1983:III-C-1) The Earth's magnetosphere results - that region of space that is dominated by the Earth's magnetic field rather than the Solar wind. The magnetosphere has a teardrop shape - with the blunt end towards the Sun. Away from the Sun is the drawn out tail of the magnetosphere, called the magnetotail. See Figure 1. The dynamics of the magnetosphere is a subject of much current research, but it appears that solar wind particles are able to enter the magnetosphere in several ways.

One of the ways is by diffusion into the magnetotail. Far from the Earth, where the field lines grow indistinct, the thermal energy of the particles causes them to diffuse into the magnetotail. Particles can enter the tail and then be conducted back towards the Earth. The field lines that

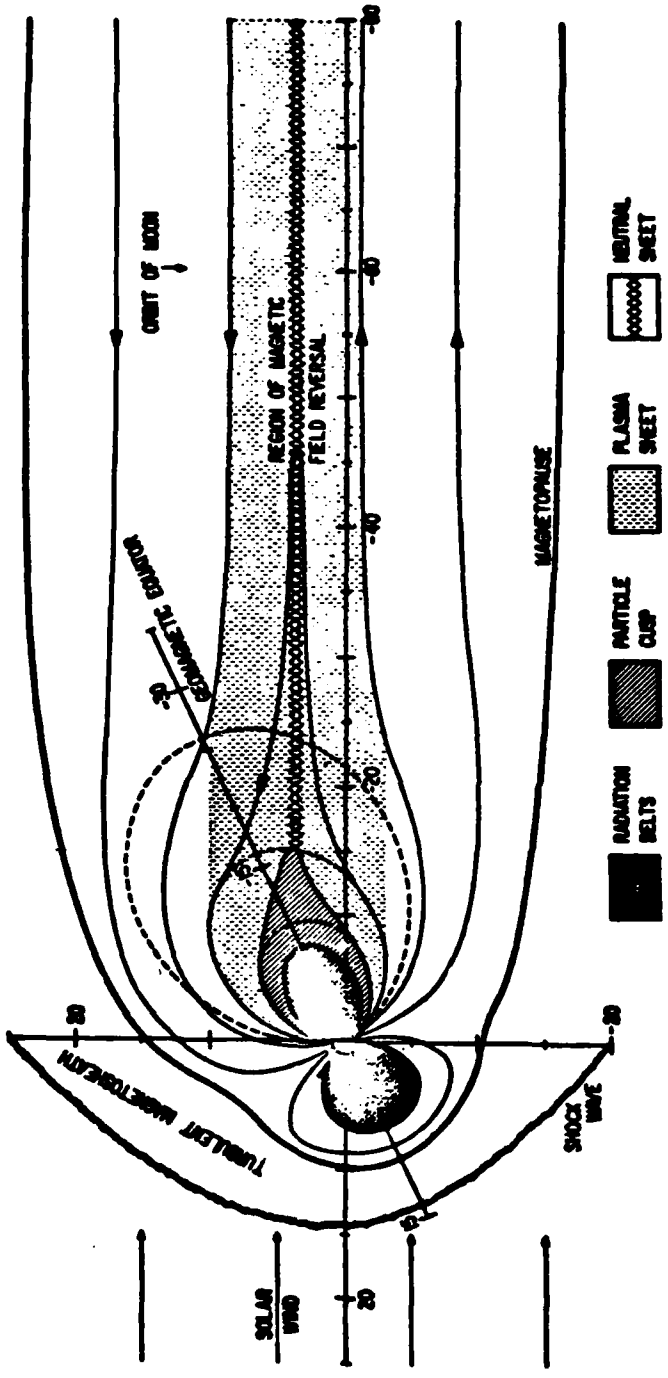

The Earth's Magnetosphere

comprise the magnetotail originate in the polar regions, but particles in the magnetotail can end up in the magnetosphere above the polar or equatorial regions. This will be discussed in subsequent paragraphs.

Another way the solar particles apparently enter the magnetosphere is through an interaction between the solar magnetic field (as carried by the solar wind) and the Earth's magnetic field. When the solar wind's magnetic field has the proper orientation, particles can be pumped directly into the magnetosphere. (Lange, 1983:IV-C-21)

Magnetospheric Particles Motion

The drawn-out magnetic field and a cross-tail electric field produce a sunward (EXB) drift on charged particles in the magnetotail. The source of this cross-tail electric field is the solar magnetic field moving past the terrestrial magnetic field. The EXB drift predominates in the outer part of the magnetotail, and drives particles toward the Earth.

As a particle gets close to the Earth, it begins to be affected by the drift produced by the gradient in the magnetic field, hereafter referred to as the grad B drift. This drift is due to the increasing magnetic field of the Earth, and drives particles around the Earth (they move parallel to the magnetic equatorial plane). Energetic particles of different charge are driven different ways by the grad B drift - electrons go eastward while ions go westward. The energy of the particles also affects how they are affected by the grad B drift. The lowest energy (slowest)

particles will not feel a rapid change in field strength, the highest energy particles will not be in the field long enough to be affected much. Mid-energy particles will be deflected most.

At the same time, particles begin to feel the co-rotation drift. This is due to the rotating magnetic field of the Earth. For electrons, this drift is in the direction of the grad B drift but for ions it is in the opposite direction from the grad B drift. Lower energy ions will get moved around quite a bit, but the higher energy ions will be less affected. The highest energy ions may just zip through the magnetic field without too much deflection (Ejiri, 1978:4808).

The different drifts have different effects on the two differently charged particles. For electrons, the grad B drift and the co-rotation drift are complementary, but for ions, they are competitors.

Particles which are not lost in the near-Earth magnetosphere (as described in the following paragraphs) will eventually move out through the dayside magnetopause (Gussenhoven, 1983:5700).

The Near Earth Magnetosphere

The magnetosphere close to the Earth can be divided into two regions. The first is a transition from the drawn-out magnetotail to the complex near-Earth environment, and the second is the near-Earth structure. A rough point to divide the two regions would be at a distance equal to six times the

radius of the Earth (Lange, 1983:III-D-3). This point is mentioned to establish the scale of the magnetosphere on the night side of the planet. There are many effects of charge and magnetic activity that will vary the determination of the region of transition's location.

The transition region's fields are a nearly perpendicular electric and magnetic field, while the near-Earth structure is an approximately dipole magnetic field (Glasstone, 1965:521) and a very complex electric field. In the far magnetotail, the magnetic field lines are faint and nearly straight and parallel. Closer to the Earth, the field lines grow stronger and begin to curve. Some particles follow the field lines and are conducted into the polar magnetosphere, and some cross the faint field lines and penetrate closer to the Earth. Those which continue towards the Earth will begin to encounter the first closed field lines. Some will again continue to cross the field lines and some do not - they begin to follow the field lines. One of the mechanisms used to explain which particles do what is the idea of "pitch angle diffusion". Each particle, in its random motion, has a velocity component normal to the closed field lines and one parallel to the closed field lines. Assuming that the particle has been traveling Earthward from the tail - when it encounters a closed field line, the line is approximately perpendicular to the magnetic equator. The particle's total velocity will be at some angle from the field line. If the angle is "small enough" (depending on local conditions) the

particle will follow the field line. In general, there is a cone about the field line, such that if the total velocity vector of the particle lies within it, the particle will follow the field line rather than continuing Earthward.

The structure of the near-Earth magnetosphere is very complex. It is dominated by the nearly dipole magnetic field of the Earth, and confined within a region by the flowing Solar wind. The magnetic field is very dynamic, changing in response to the Earth's many motions. For instance, as the Earth moves in its orbit, the two poles are moved alternately closer to the Sun. There are certainly differences (many not yet defined) between the summer and winter magnetosphere. One effect evident in the spacecraft data (Hardy, 1979:43) is photoelectrons generated in the summer hemisphere that follow the magnetic field lines into the conjugate hemisphere. Certainly there could also be some differences between the North and South poles due to the opposite directions of the magnetic fields. There are major differences in the dayside of the magnetosphere and the nightside: the largest being that the dayside is compressed while the nightside is extended.

There are three features of the magnetosphere that require description in this thesis. The first is the aurora itself. The auroral zones are bands that encircle the magnetic poles. They can be represented during quiet times by a circle whose center is offset from the magnetic pole toward the midnight sector by about four degrees. (Hardy, 1979:13)

The width in latitude of these bands is very difficult to quantify under many conditions, so this thesis and the studies it is based on have concentrated on the equatorward edge of precipitation - which is more readily identified than the polar edge. The auroral zones lie under the most polar of the closed magnetic field lines. (Spjeldvik, 1983:16) At this point one should note that the aurora can be divided into two types: diffuse and discrete. The two types are well named - the diffuse aurora is an even, low intensity glow, where the discrete aurora is a bright, highly structured display. The discrete aurora is the visible aurora seen by observers at high latitudes, and is generally coincident with, and extends more toward the pole than, the diffuse aurora. See Figure 2. This is a DMSP auroral image taken over the northern polar cap on 10 January 1983 from about 1530 to 1550 UT. Most of the nightside half of the auroral oval is imaged. Local midnight is on the left of the image, local dawn is to the center-bottom, and local dusk is at the center-top. City lights in eastern Russia lie underneath the dusk oval and burning oil fields can be seen in the upper left hand corner. The diffuse aurora, lying at the equatorward edge of the oval, is evident - especially in the upper left hand corner. Discrete arcs can be seen on the poleward edge (this is typical) with two distinct westward traveling surges visible in the lower left. The visible auroral displays are caused by charged particles cascading down into the atmosphere and reacting with high altitude atoms and molecules. These

Figure 2. The Aurora

charged particles have followed magnetic field lines from further out in the magnetosphere. It is very important to understand that if the aurora lies under the most polar of the closed magnetic field lines, then an understanding of the behavior of the auroral zones will give direct evidence of the conditions out in the magnetosphere at the limits of the closed field lines. It is also very interesting to note that the polar edge of the auroral zones, though sometimes well defined, is generally much more difficult to find in precipitation data. The equatorward edge is usually a well defined line.

It is shown, in this paper as well as many others, that the behavior of the equatorward edge of the auroral oval can be correlated with the change of the magnetic field of the Earth.

One point where the auroral zones have an interesting feature that must be mentioned in where the open and closed field lines separate on the day side of the planet. This is known as the "cusp" and there is one in each pole. These points are of considerable interest since they may be points where charged particles find easy access to very near the Earth. From spacecraft data, it appears that the auroral zones are very disordered in the area of the cusp. Of course this quick description omits many points, some of which will be covered in subsequent paragraphs.

One final description in this section is of the Van Allen belts. Discovered in 1958, they have been shown to be a

region of trapped low to high energy electrons and ions which have two major superimposed motions that act to carry them around the Earth. One is the previously described Grad B drift, caused by spiralling around magnetic field lines in a region of a fairly consistent magnetic field gradient. The other is a bounce motion, where the charged particles follow the magnetic field lines into the high latitude regions but are then reflected by the increasing magnetic field. (Glasstone, 1965:548) They then "bounce" back and forth between the poles while at the same time circling the Earth. The Van Allen belts so form a current around the Earth which greatly complicates the electric and magnetic fields. The Van Allen belts also appear to be the fate of many of the particles conducted Earthward from the magnetotail that are not lost in precipitation. The intimate connection of the auroral zones and the Van Allen belts assures us that a better understanding of the aurora will shed considerable light on the Van Allen belts.

III Literature Review

This thesis grows out of a continuing series of studies of the auroral regions by researchers at the Air Force Geophysics Laboratory. A brief review of the progress applicable to this study that they have made in understanding auroral precipitation and its relationship to the structure of the magnetosphere is appropriate at this point.

The first paper that is a major source of methodology (and inspiration) for this thesis is Hardy (1979). In it, the format of the data as analyzed in the thesis was introduced, and the criteria for determining the corrected geomagnetic latitude (CGL) of the auroral boundary was established. It connected earlier analyses of images of the aurora to the analysis of precipitation data. This paper analyzed electron precipitation in the dawn and dusk regions of the auroral zones.

A later paper, "DMSP/F2 Electron Observations of Equatorward Auroral Boundaries and Their Relationship to Magnetospheric Electric Fields", related the apparent connection between the equatorward boundary of the auroral oval and the dynamics of the position of the inner boundary of the plasma sheet. The radial distance of the inner edge of the plasma sheet determines the equatorward boundary of the auroral oval (Gussenhoven, 1981:768). This paper reported the results of using linear regression to examine the relationship between the CGL of the auroral boundary and the

magnetic activity of the Earth as measured by the Kp index. For this analysis, the boundaries were divided into hour bins by assigning each measured boundary to a bin determined by the hour in which the boundary occurred. It was found that Kp orders the equatorward auroral boundaries linearly throughout the entire range of values of Kp (Gussenhoven, 1981:773), and that there is a negative linear relationship - the auroral oval expands to lower geomagnetic latitude with increasing magnetic activity. This paper also related the auroral equatorward boundary with the last closed equipotential electric field line, through the zero energy Alfven layer. It is shown that the equatorward boundary of the auroral oval "maps" to the last closed equipotential surface in the magnetosphere (Gussenhoven, 1981:775). A conclusion drawn in this paper was that for quiet times the electron auroral boundary can be represented as a circle of radius 21 degrees, centered at 88.0 degrees on the 0240 MLT (Magnetic Local Time) meridian (Gussenhoven, 1981:775).

A new satellite, DMSP/F4, offered the opportunity to extend the earlier work into new hours. Its orbit, which covered the noon/midnight meridian, extended the available magnetic longitudes in which precipitating electrons could be measured. Here also, change in precipitation pattern by longitudes was examined by subdividing the available measured boundaries by hour bins. A conclusion from this paper was that, for a Kp of zero, the boundary oval could be represented as a circle centered at 87.6 degrees on the 0240

MLT meridian, with a radius of 21.2 degrees. For a Kp of 5, the circle was centered at 85.8 degrees and had a 29.1 degree radius (Gussenhoven, 1983:5697). As the magnetic activity increases, the oval shifts equatorward along the 0240 MLT meridian.

Ion detectors were first flown on the DMSP/F6 satellite, and an initial study of its data also heavily influenced this thesis. In a yet to be published paper, AFGL modified the electron auroral boundary criteria to fit the ion returns, used Kp to order the ion aurora, found that the difference between the electron and ion aurora was neither higher nor lower during times of high or low Kp levels, and also found that the differences were the same in the two poles. In this study, the change in difference was quantified, leading to the idea of finding the hour bins where the differences are zero. They calculated the difference between the electron and ion aurora (electron auroral boundary latitude minus ion auroral boundary latitude) for each orbit and found a mean difference. In the morning, their analysis showed that between the 0600 hour bin and the 0400 hour bin the mean difference went from -3 degrees to about -2 degrees. Here a negative sign indicates that the ion aurora is poleward of the electron aurora. On the evening side of the planet, the difference from the 1700 hour bin to the 2000 hour bin went smoothly from about +1.7 degrees to about +0.7 degrees. In the hours of coverage for the F6 satellite, the difference shows a progression from higher to lower separations.

IV Data Source and Preparation

Satellite Orbit

The DMSP/F7 satellite is in an 835 kilometer near circular polar orbit. The orbit has been set up so that the satellite's orbit plane precesses around the Earth once per year. This is referred to as a sun-synchronous orbit, and allows the satellite to keep the same sun angle on the ground below it at all times. Another way of saying that is that the satellite remains in the same local time zone on every ascending pass. The F7 satellite covers the "1000 - 2200 meridian" - it always sees the 1000 time zone on the dayside of the planet and the 2200 time zone on the night side. The satellite's orbital period is approximately 101 minutes.

Due to the 11 degree difference between the Earth's spin axis and the magnetic axis, the satellite sees a small range of magnetic local times. Figure 3 shows the orbital position of the satellite projected down the magnetic field lines to an altitude of 110 kilometers using a Jensen-Cain magnetic field model.

The satellite orbit introduces some bias into the results, giving more boundary crossings in periods of low magnetic activity. This is due to the expansion of the auroral zone in times of high magnetic activity and contraction in times of low activity. As an illustration - look at the 00 MLT line on figure 3. If, during a time of

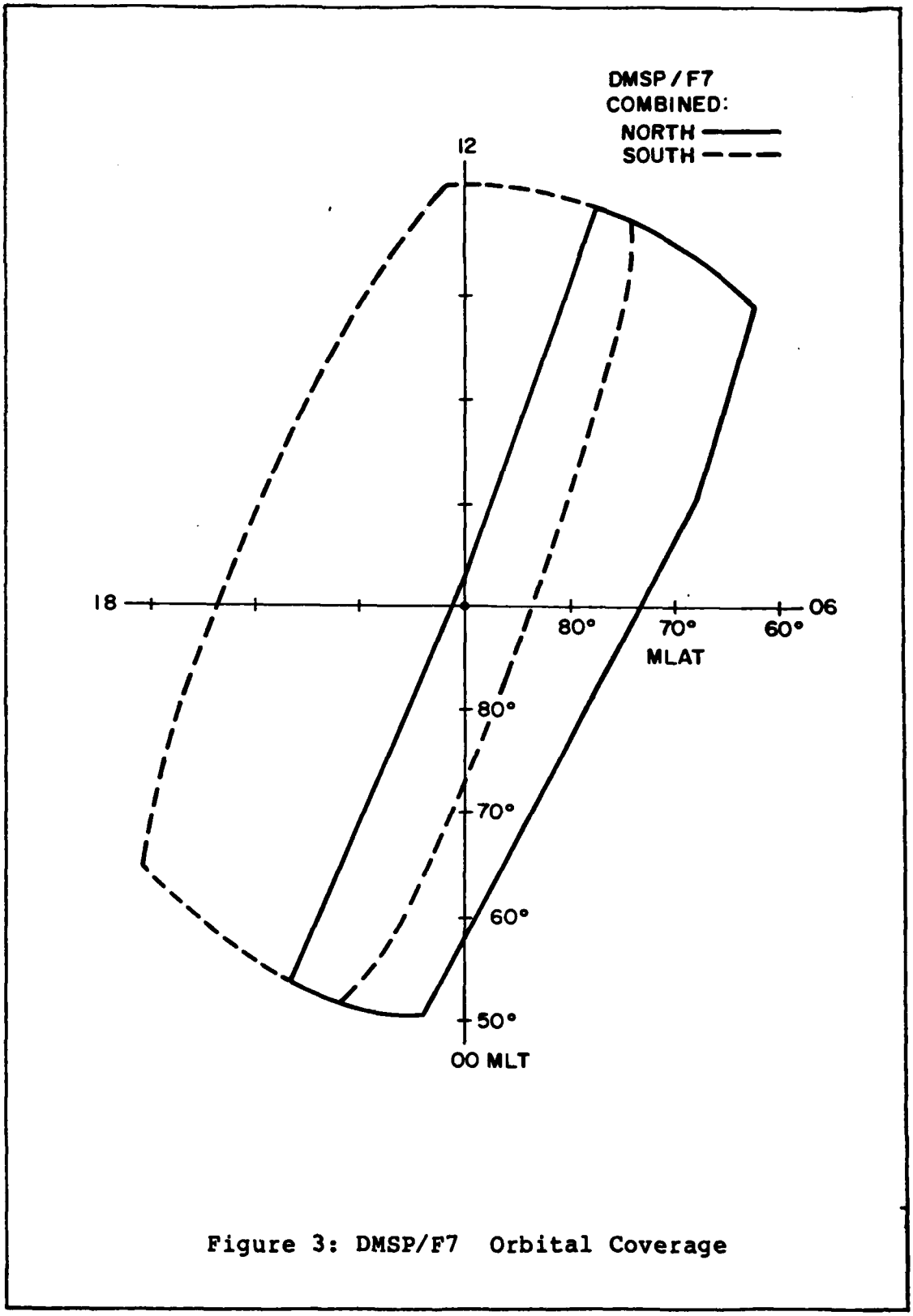

Figure 3: DMSP/F7 Orbital Coverage

low magnetic activity the auroral boundary was at 60 degrees in the north pole, the satellite would see the boundary. If, as magnetic activity increased, the boundary moved out to 55 degrees, the satellite would no longer be able to measure the boundary. This simplified example illustrates how there would be more boundaries in this time zone during times of comparitively low magnetic activity.

The DMSP satellites are non-spinning, and the sensors are mounted so that their look directions are oriented radially outward from the earth at all times. This ensures that they measure precipitating particles only, and not trapped or backscattered particles (Gussenhoven, 1982:5693)

Instrument

The following description of the sensor is taken nearly verbatim from Hardy (1984a and 1979). The electron and ion spectrometers (referred to as Special Sensor J/4) on the DMSP/F7 satellite measure the flux of electrons and ions in 20 energy channels in the range from 30 ev to 30,000 ev. This is done using a set of four cylindrical curved plate electrostatic analyzers arranged in two pairs, shown in figure 4. Each analyzer consists of three basic components: an aperture, a set of two concentric cylindrical curved plates, and a pair of channeltrons. The aperture collimates the incoming particles, defining the solid angle for particles (electrons and ions) to access the space between the cylindrical plates. A symmetric potential is applied to

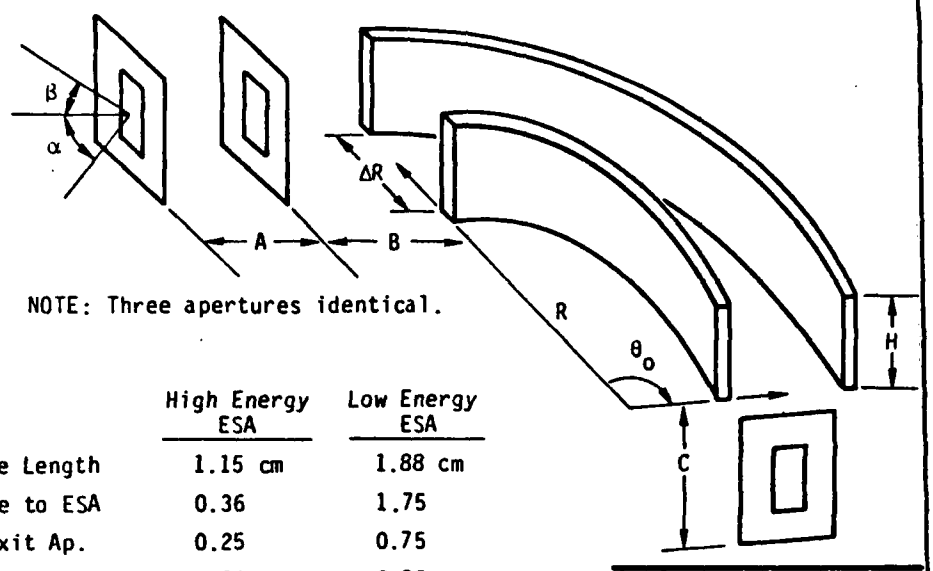

NOTE: Three apertures identical.

	High Energy ESA	Low Energy ESA
A - Telescope Length	1.15 cm	1.88 cm
B - Telescope to ESA	0.36	1.75
C - ESA to Exit Ap.	0.25	0.75
H - Plate Height	2.85	2.85
ΔR - Plate Separation	0.25	0.75
R - Mean Plate Radius	10.01	3.00
θ_o - Plate Arc	60°	130°
Aperture Width	0.20	0.20 (Electron) 0.51 (Ion)
Aperture Height	1.80	0.60 (Electron) 1.59 (Ion)
Detectors, Cone Dia.	1.09	0.38 (Electron) 1.09 (Ion)

Detector Detail

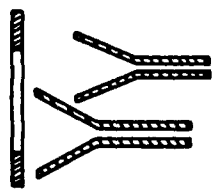

Figure 4. Electron/Ion Spectrometer (SSJ/4)

the plates creating an electric field such that particles entering the space between the plates are accelerated toward the inner plate. If the incoming particle's energy is such that the applied electric field curves the particle trajectory with a radius of curvature just equal to the average radius of the curved plates, the particle impacts the front end of the channeltron and is counted. Both electron and ion detectors use post acceleration (100 volts electrons; 1000 volts ions) to insure unit channeltron efficiency at low energies. The analyzers for ions and electrons are identical except that the polarity on the plates is opposite and the low energy ion aperture is larger than the low energy electron aperature.

Each pair of analyzers consists of one set of cylindrical plates subtending an arc of 60 degrees and another set subtending an arc of 127 degrees. The 127 degree detector measures electrons or ions in ten channels spaced logarithmically in energy between 30 and 1000 ev. The detector dwells for a period of 98 milliseconds in each channel; 2 milliseconds being left between steps to stabilize the voltage. The plates sequence from high voltage to low. The 60 degree analyzer measures electrons or ions similarly in 10 channels between 1 keV and 30 keV. The two analyzers are stepped together such that a complete 20 point electron and ion spectrum is measured once per second.

Calibration

The data returned by the DMSP/F7 detectors is displayed as plots of three quantities over time: JTOT, JETOT, and EAVE. JTOT is the total number flux of particles, or integral flux. JETOT is the integral energy flux, or just the total number flux with the energy of each channel multiplied in. EAVE, the average energy, is the ratio of the two, and represents a total average energy across all 20 channels.

Below is the equation for the first of these quantities:

$$JTOT = \sum_i j(E_i)\left[\frac{E_{i+1} - E_{i-1}}{2}\right] \qquad (1)$$

where $j(E_i)$ is the differential flux for each energy channel i, with central energy E_i. The formula for $j(E_i)$ is:

$$j(E_i) = (C_i/\Delta T)/\left[G(E_i)\Delta E\right] \qquad (2)$$

with C_i, the counts in the interval ΔT; $G(E_i)$, the energy dependent geometric factor; and ΔE, the width of the energy range for that channel i. The two quantities JETOT and EAVE are found from:

$$JETOT = \sum_i E_i\ j(E_i)\left[\frac{E_{i+1} - E_{i-1}}{2}\right] \qquad (3)$$

$$EAVE = \frac{JETOT}{JTOT} \qquad (4)$$

Many of these sensor performance quantities are incorporated into the sensor design. Once the sensor is built, however, these performance quantities must be measured

during tests at ground based facilities with calibration sources of particles. Of those that must be measured, the first is the energy dependent geometric factor of the detector, $G(E_i)$. It represents the effective aperture size at each energy of incident particles. The second is the width of the energy band that is measured at each energy, ΔE_i. This tells the spread in energy of the particles at each energy that will be measured. The last quantity, E_i , is the actual peak energy of maximum transmission by the curved plate analyzer given a certain plate voltage.

These numbers were measured for two detectors identical to the DMSP/F7 detectors at the Air Force Geophysics Laboratory, (Hardy,1984a) and are applied to the F7 detectors. The calibration effort for these detectors has quite a history. For earlier detectors, calibration facilities at Rice University and the Southwest Research Institute were used, with mixed results. But it does appear that the detectors are very similar in response and derived numbers for one detector can be used for another.

The following description is taken largely from Hardy, (1984a and 1979). All three calibration facilities use basically the same technique for producing an electron beam: an aluminum surface is floated to a high negative potential and illuminated with a monochromatic ultraviolet source. A ground screen is placed in front of the metal surface such that the photoelectrons produced by the ultraviolet are accelerated away from the surface, producing the beam. The

instrument to be calibrated is mounted on a fixture such that the look direction of the detector can be positioned at any angle desired relative to the beam. The system produced a homogeneous beam of particles with an approximatly 18 inch radius, tunable in energy from about 30 volts to 35,000 volts. The entire system is contained within a set of Helmholtz coils used eliminate particle motion effects caused by the Earth's magnetic field.

The calibration system is computer controlled so that it automatically sequences through a two dimensional array of angles relative to the aperture for any fixed energy of the incident beam. The counts accumulated as the detector dwells at each angular position are stored in core and recorded onto magnetic tape, The current density in the beam is determined using a Faraday cup that is shifted into the beam at the beginning of each angular scan.

At the end of each scan the computer calculates the energy dependent geometric factor, $G(E_i)$. By determining $G(E_i)$ at a series of energies one can approximate the response curve for each fixed voltage on the plates. The response curve allows one to determine the channel pass band, ΔE. By using the value of $G(E_i)$, and the known counts in the channel, C, and the accumulation interval, ΔT, one can find $j(E_i)$ by the formula,

$$j(E_i) = C/\Delta T \; G(E_i) \Delta E_i \qquad (5)$$

Boundary Selection

The measured flux levels are analyzed by printing them in the format shown in Figure 5. This example shows the raw data plots for electrons (top) and ions (bottom) during a north polar pass of the F7 satellite on 16 December 1983. The flux is shown in three plots per panel - integral flux (JTOT) on the bottom, energy flux (JETOT) in the middle, and average energy (EAVE) on the top. The horizontal axis is labeled with the number of seconds since the beginning of the day in Universal Time. This pass begins at 0658 UT (25080 seconds) and ends at 0720 UT (26400 seconds). The values of JTOT, JETOT, and EAVE are derived from equations 1, 3, and 4 respectively and the measured values of $j(E_i)$. JTOT and JETOT are plotted on logarithmic scales; the values for average energy are plotted on a linear scale. Below each set of three plots, at two minute intervals, ephemeris points are given. The points given are the geographic coordinates of the satellite (GLAT and GLONG), the corrected geomagnetic coordinates of the satellite (MLAT and MLONG), all of which are projected along the magnetic field line to 110 kilometers altitude, and the magnetic local time (MLT).

The auroral zone has been shown (Hardy, 1979:32) to be indicated by a rise in flux levels above the level of the general background. Diffuse aurora show up as a steady level in JTOT, while discrete aurora appears as very irregular peaks. There are two sources of error that should be noted at

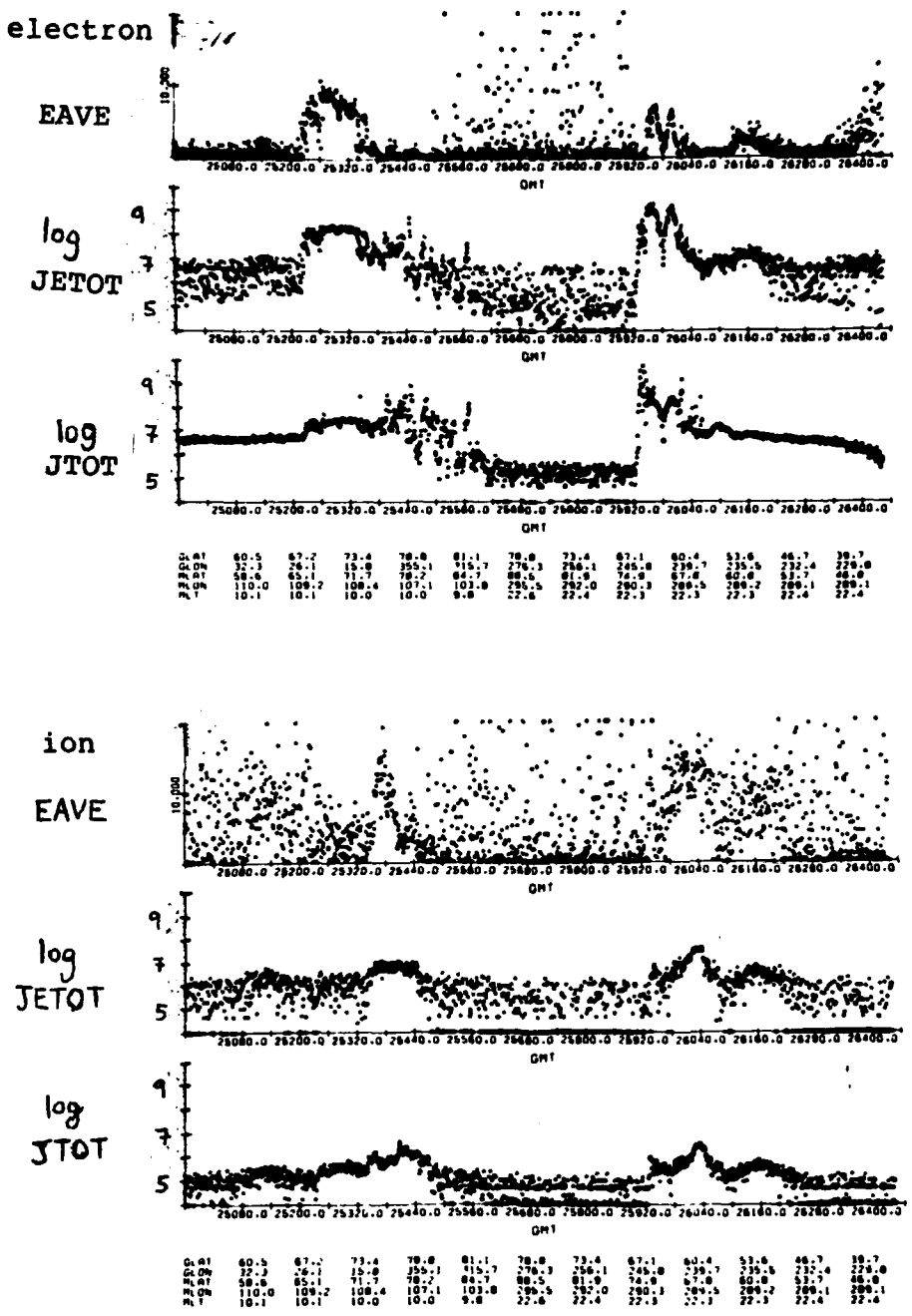

Figure 5. Format of F7 Flux Plot

this point - photoelectrons from the South Pole and radiation belt particles. Both of these will be detected as well as the precipitating particles and show up as a rise in flux above the background. Photoelectrons will appear to be a broad "ramp", and only show up in the electron panel, while radiation belt particles show up as rounded humps in the flux level (Hardy, 1979:32). Radiation belt particles often appear equatorward of the auroral zones in both electron and ion panels. With this brief introduction, four example data points will be determined.

The morning electron diffuse auroral boundary is at 0700:30, where a sharp rise in JTOT begins. This rise is also apparent in JETOT and EAVE. The steady value indicates that it is diffuse aurora. The satellite geomagnetic latitude (projected to 110 kilometers) is 60.2^{o} , and its geomagnetic local time 1000. This point would join the others in the 1000 hour time bin, flagged as a North Pole electron boundary. The discrete aurora begins at about 73.3^{o} , as indicated by increased scatter in the flux level. The polar cap is very quiet, and just appears as a flat area of low precipitation. The aurora reappears with the sharp rise in flux levels at about 74.9^{o} . Here the flux indicates mixed discrete and diffuse aurora. Some ambiguity can be seen next, as the flux levels in JETOT and JTOT do not show clear changes at the same latitudes. It appears that JETOT does not return to background levels until about 59.0^{o} , a point where there is not a clear change in JTOT. However, there is a definite drop

in EAVE at that point. Examining the three plots, and comparing them to the ion panel, it can be seen that the rise below 66.1° has a very regular humped shape which is repeated in the ions. This apparently is radiation belt contamination. The equatorward boundary recorded is 66.1° and its magnetic local time (MLT) bin is 2200.

The ions show similar features, but tend not to have the sharp changes seen in electron fluxes. Looking at the ion panel, there is somewhat of a rise, centered at about 61.9° , after which the flux returns to background levels. It rises again at about 66.8° for an extended time. The rise centered at 61.9° is apparently radiation belt contamination. The equatorward diffuse auroral boundary would be logged as 66.8° in the 1000 MLT bin. The ionic polar flux is again featureless, with the flux rising at about 74.9°. The flux rises to a maximum and begins to drop, with a low point at about 66.9° . The following rise has the humped appearance of radiation belt particles and should be ignored. The boundary is logged at 66.9° in the 2200 MLT bin.

This procedure has been repeated for each survey plot, and resulted in the data file used in this study.

Some features of the aurora should be noted at this point. First, the aurora does seem to form bands encircling the poles rather than continuous caps or thin rings. Second, the equatorward boundary for electrons and ions occurs in the same magnetic local time bin in the North and South poles - 1000 in the morning and 2200 in the evening. This is very

common. And finally, the ion auroral boundary is considerably higher (6.6° higher) than the electron boundary in the morning, while the two boundaries are very close in the evening. These observations will be shown to have meaning in later chapters.

Data Sources

Data used in this study comes from three different sources. Precipitation data is from the DMSP/F7 satellite, courtesy of the Air Force Geophysics Laboratory, Space Physics Division, Hanscom, AFB, Massachusetts. In order to extend the amount of time covered by this study, only every other orbit of the satellite was considered. This reduced the number of boundaries in each day, but allowed the inclusion of orbits from the first nineteen days of December 1983. Additional coverage was obtained by using data from an earlier study (Hardy, 1984a), which looked at similar data from the DMSP/F6 satellite. F7 data provides coverage in the 0700 - 1100 and the 1900 - 0000 hour bins. F6 data is in the 0300 - 0700 and the 1500 - 2000 hour bins.

The source for the values of Kp was the International Service of Geomagnetic Indices (IUGG). Three hour averages of Kp from the worldwide magnetometer network were taken as the Kp values for those three hour spans.

The ap values are from the Air Force Global Weather Central (AFGWC) magnetometer network. Again, three hour average values of ap were taken as the ap value for the three

hour span. These values are potentially useful since, unlike the ap values available from the IUGG, they are available in near-real time from AFGWC.

V Methodology

Linear Regression

Regression is a general statistical technique through which one can analyze the relationship between a dependent variable and an independent variable. Regression may be viewed as a descriptive tool by which the linear dependence of one variable on another is summarized and decomposed. This study uses linear regression to study the relationship between the magnetic activity of the Earth (as measured by the Kp index), and the latitude of the equatorward boundary of the diffuse aurora.

In bivariate (one independent variable, one dependent variable) regression analysis, values of the dependent variable are predicted from a linear function of the form

$$Y' = A + BX \qquad (6)$$

where Y' is the estimated value of the dependent variable Y, B is a constant by which all values of the independent variable X are multiplied, and A is a constant which is added to each case (Nie, 1975:323).

The difference between the actual and estimated value of Y for each case is called the residual and may be represented by the expression, residual = $Y - Y'$. The regression strategy involves the selection of A and B in such a way that the sum of the squared residuals is smaller than any possible alternative values. Expressed mathematically, $\sum(Y - Y')^2$ is

a minimum.

It is possible to find the best values for A and B by finding the mean values for the quantities X and Y and then manipulating sums of differences between the means and individual data points. The optimum values for A and B are obtained from the following equations:

$$B = (X - \langle X \rangle)(Y - \langle Y \rangle)/\sum(X - \langle X \rangle)^2 \qquad (5)$$

$$A = \langle Y \rangle - B\langle X \rangle \qquad (8)$$

where first the individual differences between each value of X and its mean value <X> are found, the differences between each value of Y and its mean value <Y> are found, and the differences are manipulated as indicated (Nie, 1975:323).

The constant A (referred to as the Y intercept) is the point at which the regression line crosses the Y axis and represents the predicted value of Y when X = 0. The constant B, usually referred to as the (nonstandardized) regression coefficient, is the slope of the regression line and indicates the expected change in Y with a change of one unit in X. The predicted Y' values fall along the regression line, and the vertical distances (Y - Y') of the points from the line represent residuals (or errors in prediction). Since the sum of squared residuals is minimized, the regression line is called the least-squares line or the line of best fit.

The "goodness of fit", or how well the regression line predicts the data, is measured by the quantity "cc", or

correlation coefficient. This value will be close to one for a good fit and close to zero for a poor fit. This value appears in all tables of regression results in this thesis.

In this study, the appropriate form of Equation 6 is:

$$\lambda = \lambda_0 + \alpha Kp \qquad (9)$$

where:

λ = the estimated corrected geomagnetic latitude of the equatorward diffuse aurora, the dependent variable.

λ_0 = the predicted value for the latitude of the boundary at Kp = 0.

α = the slope of the regression line.

Kp = the geomagnetic activity of the Earth as measured by the Kp index, the independent variable.

The data used in this study is many measured values of the latitude λ of the auroral boundary and Kp, with the object being to find values of λ_0 and α and compare them based on the way the sample data was subdivided.

The regression equations found are only valid for the span of Kp or ap that was used in this study. The equations are valid at zero levels of the indices, but not at the highest possible values.

Data Subdivisions

Based on earlier studies, it appears that the different forces on particles in the magnetosphere will cause gradual changes in the precipitation patterns in different

geomagnetic longitudes. The object of this part of this study is to find the best one of several different ways of subdividing the measured boundaries. The orbital coverage of the satellite naturally divides the available data by pole and by morning and evening, and the two detectors divide the data by charge. But should the data be further subdivided?

The first strategy employed was to group the data into eight "bins" by the above natural division. These eight bins are divided by North Pole versus South Pole, by evening versus morning, and by electron versus ion. The results from these bins can be compared to reveal the patterns from bin to bin.

The second subdivision broke those categories down further. The new "hour bins" are the boundaries divided by their magnetic local time of occurence. For instance, all boundaries that occurred between 0900 and 1000 were grouped as the 0900 hour bin. The results from these bins can be compared, and any conclusions can be compared to conclusions drawn from the earlier subdivision.

With each subdivision, the results should be more valid for a specific geomagnetic longitude, but the sample size is smaller. To keep the sample size high enough to be meaningful, it is advantageous to aggregate the measured boundaries in a way which does not conceal the true effect of the magnetospheric forces on that geomagnetic longitude. One possible way to do this is to pool the measured boundaries from the two poles. The results and conclusions drawn from

them should be statistically more meaningful and still valid for a small span of geomagnetic longitude.

Finally, it is possible to separate measured boundaries by time of year. Based on the changes in the orientation of the magnetosphere with respect to the solar wind over the span of one year, it may not be valid to pool (for instance) spring and summer measurements.

The General Linear Test

The test used here to determine if regression lines are equivalent is the General Linear Test. This test will tell if, within a set tolerance, the intercepts and slopes of the regression lines are the same. The "null" hypothesis (what the test should prove) will be that the lines are the same. This can only be if the two intercepts and the two slopes are the same. The alternative hypothesis is just that the two lines are different. If the test finds that the two lines are different, it may be that the intercepts or the slopes are different or that both are different. The test will not say which one is the case.

This test is set up to test the "full model", or the data points run in separate regression routines, against the "reduced model", or the data pooled in a single regression run.

At this point, it is appropriate to introduce two new terms. The "Error Sum of Squares", written as SSE, is a sum of differences. It is arrived at by (for instance)

calculating the mean value of the equatorward boundary of the aurora for a population, and then finding the difference between each measured boundary and the mean. Some of these differences will be positive and some will be negative, so each difference is squared and all are summed. The equation for SSE is (Neter, 1974:45):

$$SSE = \sum (Y - \langle Y \rangle)^2 \qquad (10)$$

This number is produced by the SPSS package for each regression run. The "degrees of freedom" for a linear regression equation is the number of data points used in that equation. This number indicates the number of sources of error in the regression equation. The degrees of freedom are written n_0, where the subscript refers to the regression line's data population. A zero would indicate the degrees of freedom being referred to were those of the zeroth data population.

The General Linear Test proceeds in steps. First, run regression for the full model (separate groups) and obtain the error sum of squares SSE(F), this value is found by summing the error sum of squares for each individual regression line. Then run regression on the reduced model (pooled groups) and obtain the reduced model error sum of squares SSE(R). Last, calculate the F^* statistic which involves the difference between the two error sums of squares, SSE(R) - SSE(F). Compare this to the F statistic from tables at the chosen level of significance (Neter, 1974:

161). The F statistic is found from Neter (1974:164):

$$F^* = \left[SSE(R) - SSE(F)/2\right]\left[(n_1 + n_2 - 4)/SSE(F)\right] \quad (11)$$

The degrees of freedom of the two regression lines are taken into account by the two terms: 2 and $n_1 + n_2 - 4$ in the equation for F^*. The 2 is a necessary correction factor for the equation which compares 2 regression lines.

Processing Equipment and Software

One consideration in the preparation of the data was the processing equipment and statistical software that would be employed for analysis. In this project, processing equipment consisted of a CDC Cyber 6000 computer located at Wright-Patterson AFB, Ohio. This CDC system is shared by the Air Force Institute of Technology with other Air Force units. The software used in this study was a version of the Statistical Package for the Social Sciences (SPSS), developed by Northwestern University's Vogelback Computing Center. The SPSS program was selected for the project because of its wide use at AFIT, its superior documentation, and its high level of user friendliness.

VI Results

Analysis of Auroral Boundary Behavior

This part of the analysis compared the auroral equatorward boundary to the magnetic activity of the Earth. The goals have been to determine how best to group the data and to see if the magnetic index ap (as reported in near-real time by AFGWC) can be used as well as the Kp index (which comes out more slowly). The study will explore whether the north and south polar boundaries can be combined, which depends on whether the north and south polar aurora are symmetric at this time of year.

In this section, a large number of measured auroral boundaries and the Kp or ap index for that time are used to generate a predicted minimum boundary (called λ_0) and a predicted mean increase (or response) in the auroral boundary latitude (called α). These λ_0 and α values are tabled along with the correlation coefficient , the number of points used, and the significance of that run. The significance value can be considered the probability that the result occurred by chance. The equation that these values are from is:

$$\lambda = \lambda_0 + \alpha \, Kp \qquad (12)$$

The analysis began by breaking down the data set into eight subsets. They are differentiated by the two poles, by particle type, and by the two sides of the orbit (morning and

evening). An SPSS linear regression routine gave a λ_o (corresponding to the smallest predicted auroral oval for the magnetic activity measured) and an α (corresponding to the mean change in oval size per increase in magnetic activity) for each of the eight subsets. In this section the λ_o values are referred to as "minimum boundary" and the α as the "mean increase". The results are in Table 1.

Table 1

Results of Linear Regression on Initial Boundary Grouping

	Kp			Ap			
	λ_o	α	cc	λ_o	α	cc	#
NP e- morn	70.421	-0.172	-0.6221	68.497	-0.141	-0.4321	121
" ion "	72.715	-0.132	-0.5707	71.349	-0.117	-0.4271	118
SP e- "	69.954	-0.104	-0.4715	69.389	-0.123	-0.4381	109
" ion "	73.179	-0.112	-0.4989	72.486	-0.125	-0.4559	108
NP e- even	67.454	-0.205	-0.3976	65.636	-0.198	-0.3261	123
" ion "	67.306	-0.167	-0.3342	65.853	-0.165	-0.2796	120
SP e- "	67.896	-0.183	-0.7761	66.949	-0.220	-0.7320	109
" ion "	67.571	-0.172	-0.7947	66.634	-0.200	-0.7567	108

(All significances are $\leq$ 0.01)

This table allows one to compare the electron and ion aurora at the four places where equatorward boundaries occur: North Pole morning, South Pole morning, North Pole evening, and South Pole evening. It indicates that in the morning, the ion aurora is at a higher latitude than the electron aurora, but in the evening the electron aurora is higher. This was also found in Hardy (1984b).

This table also allows one to compare morning and evening aurora. The first point to notice is that all the evening

minimum boundaries are at about 67° , but that morning boundaries are at about 70° for electrons and 73° for ions. It appears that there is more separation between the electron and ion aurora in the morning than in the evening, and morning aurora of both particle types is at higher latitudes than evening aurora. The slope values are lower for the morning, indicating a slower reaction to changes in magnetic activity.

The correlation coefficients seem to indicate that the most ordered aurora is the South Pole evening, and the next is the North Pole morning. Then comes the South Pole evening, and the North Pole evening is the least orderly.

A comparison of the correlation coefficients for the fit with Kp versus the fit with ap shows that the fit with Kp is always somewhat better. It appears that Kp provides a better linear fit than does ap.

Next, following AFGL's example, each of the above groups was broken into one hour bins. This study looked at 0700 to 1100 in the morning and 1900 to 0000 in the evening, as it was limited by the orbital characteristics of the satellite. The SPSS linear regression routine was rerun to determine a λ_0 and α , and a correlation coefficient for each hour bin. The results are in Table 2.

Table 2

Linear Regression Results On Separated Hour Bins

	MLT	λ_o	α	cc	#	sig
NP e-	0700	70.492	-0.132	-0.5812	19	0.009
	0800	72.123	-0.286	-0.7530	38	0.000
	0900	71.992	-0.268	-0.8814	18	0.000
	1000	69.284	-0.069	-0.3738	44	0.012
	2100				0	
	2200	68.212	-0.187	-0.8098	50	0.000
	2300	67.247	-0.210	-0.7896	53	0.000
	0000	67.046	-0.138	-0.7095	20	0.000
NP ion	0700	71.638	-0.131	-0.7268	30	0.000
	0800	76.040	-0.279	-0.7190	27	0.000
	0900	73.586	-0.118	-0.5596	16	0.024
	1000	72.357	-0.074	-0.4407	40	0.004
	1100				0	
	2100				0	
	2200	67.403	-0.148	-0.7509	50	0.000
	2300	68.002	-0.187	-0.8204	45	0.000
	0000	67.797	-0.149	-0.7985	28	0.000
		λ_o	α	cc	#	sig
SP e-	0700				0	
	0800				0	
	0900	68.666	-0.042	-0.2524	31	0.171
	1000	70.181	-0.145	-0.6572	34	0.000
	1100	70.132	-0.099	-0.4882	16	0.055
	1900	70.677	-0.207	-0.9266	17	0.000
	2000	69.825	-0.230	-0.7968	20	0.000
	2100	67.892	-0.209	-0.9135	18	0.000
	2200	68.213	-0.222	-0.8891	30	0.000
	2300	66.488	-0.158	-0.8255	26	0.000
	0000				0	
SP ion	0700				0	
	0800				2	
	0900	72.335	-0.047	-0.2640	32	0.144
	1000	73.875	-0.169	-0.6760	21	0.001
	1100	74.187	-0.097	-0.4579	15	0.086
	1900	68.992	-0.183	-0.8897	23	0.000
	2000	69.442	-0.225	-0.7936	17	0.000
	2100	66.861	-0.169	-0.8396	20	0.000
	2200	67.744	-0.201	-0.8166	31	0.000
	2300	66.998	-0.153	-0.8151	25	0.000
	0000				0	

Examining the results, the correlation coefficients are higher. That should be the case, since the points are split into smaller groups. But since the correlation coefficients show a general improvement, and most of them are now quite high, one can conclude that the boundaries were subdivided in a way which makes physical sense.

An application of the General Linear Test for the equality of two regression lines to North Pole electrons in the evening hours shows that the population in the 2200 - 0000 hour bins cannot be combined. For this test, the null hypothesis is that the regression line generated from boundaries measured in the North Pole electron aurora between 2200 and 0100 is the same as the regression lines generated from those hour bins separately. This can only be the case if (within some tolerance or significance) the intercepts are the same and the slopes are the same. The level of significance used here was 0.95, so the decision rule at that significance, is,

$$\text{if } F^* \leq F(0.95;2;n_1 + n_2 - 4) \qquad (13)$$

then accept the null hypothesis, otherwise reject it (Nie, 1974:165). If the calculated F^* is indeed less than the F value, the lines are the same and the boundaries can be pooled. Otherwise, the measured boundaries cannot be pooled. The F^* value is 9.55 for this test, while the F value is 3.07. Therefore, the null hypothesis is rejected and the populations of the three hour bins cannot be pooled. This

test result was expected from earlier AFGL results.

Here again, the evening correlation coefficients are very high, indicating that the evening aurora is much more ordered than the morning aurora. The slope of the regression line is usually higher in the evening, especially in the South Pole. Again, the pattern of a higher electron aurora in the evening is apparent. The trend for morning aurora to be at higher latitudes than evening aurora continues.

The effect of the satellite's orbit can be seen in the differences between the hour bins that are represented in the North and South poles in Table 2.

There are a few differences between the electron and ion results in the same pole. They have remarkably similar slopes in the same hour bins - indicating that electron and ion precipitation respond similarly to changes in the magnetosphere. See Table 3. This does tend to reinforce the idea that the electron and ion loss regions move together in response to changes in the magnetosphere.

Table 3

Comparison of Regression Line Slopes

NP	MLT	e- α	cc	ion α	diff
	0700	-0.132		-0.131	0.001
	0800	-0.286		-0.279	0.007
	0900	-0.268		-0.118	0.015
	1000	-0.069	*	-0.074	-0.005
	2200	-0.187		-0.148	0.039
	2300	-0.210		-0.187	0.023
	0000	-0.138		-0.149	-0.011

SP	MLT	e-	cc	ion	diff
	0900	-0.042	*	-0.047	-0.005
	1000	-0.145		-0.169	-0.024
	1100	-0.099	*	-0.067	0.002
	1900	-0.207		-0.183	0.024
	2000	-0.230		-0.225	0.005
	2100	-0.209		-0.169	0.040
	2200	-0.222		-0.201	0.021
	2300	-0.158		-0.153	0.005

The middle column will have an asterisk if the correlation coefficient for that regression run is less than 0.5. Interestingly, one can include just one column since the correlation coefficients are so similar on both the electron and ion aurora in both poles. The runs where the correlation coefficient is low should have less reliability, but they still reflect the overall pattern of differences.

In the later papers, (beginning with Gussenhoven, 1983), AFGL has combined the data from the North and South Poles. This is an implicit assumption that the North and South Pole aurorae are symmetric. That assumption was examined by combining the hour bins where there was overlapping coverage. The results are in Table 4.

Table 4

Linear Regression Results On Combined Pole Hour Bins

	MLT	λ_0	α	cc	#	sig
electrons	0900	69.686	-0.123	-0.5361	49	0.000
	1000	69.497	-0.094	-0.4705	78	0.000
	2200	68.247	-0.202	-0.8391	80	0.000
	2300	66.926	-0.195	-0.8111	79	0.000
ions	0900	72.837	-0.075	-0.3945	48	0.006
	1000	72.796	-0.100	-0.5143	61	0.000
	2200	67.597	-0.172	-0.7755	72	0.000
	2300	67.467	-0.171	-0.8299	70	0.000

There were only a few hours where there were crossings in both poles in the same hour bins. Even with this small group, the same trends are apparent that were noticed in the earlier groups. This indicates that the behavior of the aurora is not concealed by combining the poles. But perhaps a more important table would directly compare the results of a regression run in the North Pole, the combined group, and the South Pole. This is Table 5.

Table 5

Comparison of Combined and Separated Hour Bins

			λ_o	α	cc	#	sig
electrons	0900	NP	71.992	-0.268	-0.8814	18	0.000
		both	69.686	-0.123	-0.5361	49	0.000
		SP	68.666	-0.042	-0.2524	31	0.171
	1000	NP	69.284	-0.069	-0.3738	44	0.012
		both	69.497	-0.094	-0.4705	78	0.000
		SP	70.181	-0.145	-0.6572	34	0.001
	2200	NP	68.212	-0.187	-0.8098	50	0.000
		both	68.247	-0.202	-0.8391	80	0.000
		SP	68.213	-0.222	-0.8891	30	0.000
	2300	NP	67.247	-0.210	-0.7896	53	0.000
		both	66.926	-0.195	-0.8111	79	0.000
		SP	66.488	-0.158	-0.8255	26	0.000
ions	0900	NP	73.586	-0.118	-0.5596	16	0.024
		both	72.837	-0.075	-0.3945	48	0.006
		SP	72.335	-0.047	-0.2640	32	0.144
	1000	NP	72.357	-0.074	-0.4407	40	0.004
		both	72.796	-0.100	-0.5143	61	0.000
		SP	73.875	-0.169	-0.6760	21	0.001
	2200	NP	67.487	-0.145	-0.7602	47	0.000
		both	67.597	-0.172	-0.7755	72	0.000
		SP	67.548	-0.205	-0.8391	25	0.000
	2300	NP	68.002	-0.187	-0.8204	45	0.000
		both	67.467	-0.171	-0.8299	70	0.000
		SP	66.998	-0.153	-0.8151	25	0.000

An application of the General Linear Test shows that the North Pole and South Pole boundaries in the same hour bin can be combined. For this test, the null hypothesis is that the regression lines generated from the measured auroral boundaries in the two poles are the same. The test procedure was, first, to run the regression routine on the two populations separately, and then run on a pooled population. The F values were computed, and the F values were found in the table from Neter, 1974. This procedure was repeated for each hour bin of overlapping North Pole - South Pole coverage and for particle types. The results are shown in table 6.

Table 6

Regression Line Equivalence Test Results

	MLT	F^*	F	
electrons	0900	13.706	3.32	*
	1000	2.919	3.15	
	2200	3.09	3.15	
	2300	1.51	3.15	
ions				
	0900	0.97	3.32	
	1000	2.33	3.15	
	2200	4.14	3.15	*
	2300	0.73	3.15	

This table should be interpreted that for six of eight groups, the measured boundaries can be pooled. For two, marked with an asterisk, they cannot. There is no apparent reason why those two groups failed the test, as they do not appear different in comparison to the other hour bins, so the decision has been made to accept that all the hour bins can be pooled.

From this analysis, it appears that the best way to

subdivide the measured boundaries is by particle type, and hour bin. It appears the one can combine the data from different poles with no systematic error.

With these results in hand, one can begin to draw some conclusions about the systematics of the aurora - this will be the subject of the next section.

Relationship of Electron and Ion Auroral Boundaries

In one of their later, as yet unpublished, studies (Hardy, 1984a) researchers at the Air Force Geophysics Laboratory compared the equatorward boundary of the electron and ion aurorae. Their studies have shown that the diffuse auroral boundary for electron precipitation could be represented as a circle about the magnetic poles, offset toward the post-midnight sector (Gussenhoven, 1983:5697). Also, they have shown the same relationship between the electron and ion aurora that has been brought out in this study - the electron aurora is lower on the dayside and higher on the nightside than the ion aurora, in both poles (Hardy, 1984a:3). They went on to find the mean difference in the electron and ion aurora in each hour bin, as a way of quantifying the separation between the two. This should lead to identifying the hour bins where the boundaries are farthest apart, and the hour bins where they cross. The points on the magnetic equatorial plane from which precipitation in those hour bins originates might be very good areas to examine.

This study has also looked at the separation of the electron and ion aurora, and determined how far apart the boundaries are in the hours of coverage. This was done in two different ways. The first was by calculating the differences between the latitudes of electron and ion aurora boundaries at the same point in the orbit, putting these differences into hour bins, and then determining the mean, for each hour bin, of these points. That analysis is summarized in Table 7.

Table 7

Mean Computed Auroral Boundary Differences

NP	μ	σ	#	SP	μ	σ	#
0700	-1.539	1.593	19				
0800	-3.141	1.635	32				
0900	-2.417	1.907	33		-2.417	1.907	33
1000	-2.309	1.887	59		-2.309	1.887	59
1100			0		-3.523	1.928	11
1900			0		0.806	1.294	18
2000			0		0.500	1.058	20
2100			0		-0.111	1.122	18
2200	-0.150	1.344	80		-0.150	1.344	80
2300	-1.157	1.572	75		-1.157	1.572	75
0000	-0.775	0.924	20				

Note that, where possible, boundaries from the two different poles have been combined and hence the results for those hour bins are listed under both the North pole and South pole columns.

The results show the lowest absolute values at about 2100, indicating that the electron and ion aurora are at the same latitude in that hour bin. Assuming that the North and South Polar aurorae are reasonably symmetric, a trend may be seen from 0000 in the North pole to 1900 in the South pole, where the ion aurora is at first below the electron aurora,

and then above it. This is the night side of the planet, where the aurora should be well ordered. On the morning side, the indicated separation is quite large, with the ion aurora still considerably below the electron aurora. The standard deviations are high, and may conceal just what the true relationship is. If the equatorward boundary of the diffuse aurora is reasonably circular, the dayside crossing should be at about 0900. However, the indicated separation at 0900 is far from zero. This is Figure 6.

The second way to compare the boundaries is to return to Table 2 and Table 4 and directly take the difference of the minimum boundaries as predicted by linear regression. Returning to Table 2, and subtracting the ion boundary from the electron boundary latitude, Table 8 results.

Table 8

Computed Mean Difference In Separated Hour Bins

	NP	SP
0700	-1.146	
0800	-3.917	
0900	-3.151	-3.151
1000	-3.299	-3.299
1100		-4.055
1900		1.685
2000		0.383
2100		1.031
2200	0.650	0.650
2300	-0.541	-0.541
0000	-0.751	

Again, the absolute value of the difference is least at 2000, but still large at 0900. Note that, again, where poles could be combined they have been. It is helpful to plot the derived minimum boundaries, so that the reader can see what

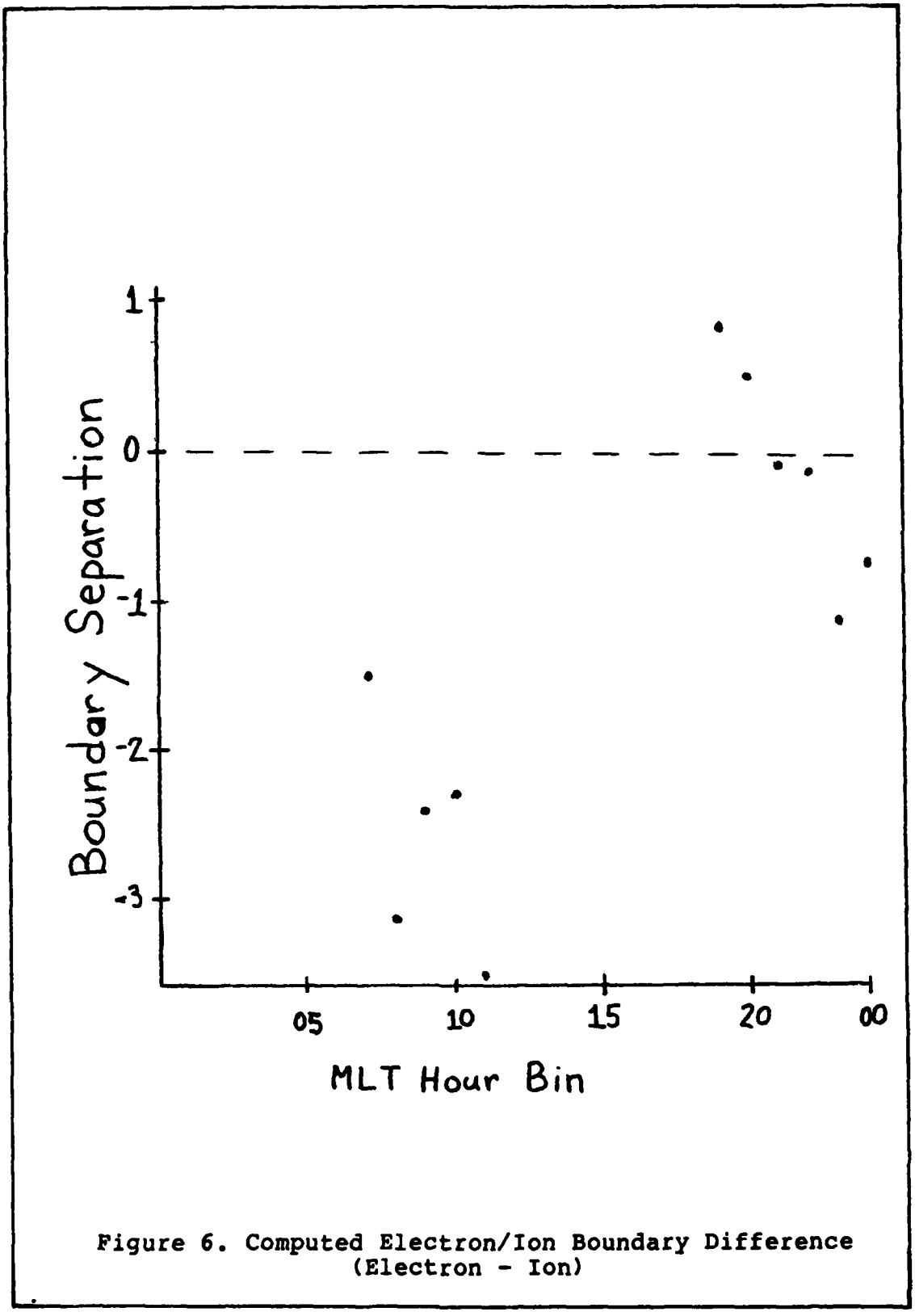

Figure 6. Computed Electron/Ion Boundary Difference (Electron - Ion)

the boundary relationship looks like as if one were above the pole looking down. The result should be two arcs about the poles. The result is Figure 7. Here, a polar plot is shown which represents the aurora as it would appear from above one of the poles. Points plotted here are from this study or from Hardy (1984b). Points from that study were also from the same time of year, so they should be compatible with points used in this study. Where possible, points generated from combined North and South pole bins have been used, but for other hours, bins representing just the North or South poles have been used. This is justified since the poles run separately produce compatible results with the poles run combined. It can be seen that the ion aurora is lower on the night side of the planet, while the electron aurora is lower on the dayside. It is also apparent that the two aurorae are very close in the 2000 - 0000 hour bins.

In an attempt to make this plot easier to read, the polar plot was transformed to a "mercator" plot. This is Figure 8. Here again, it can be seen that the electron and ion aurora are very close in the 2000 - 0000 hour bins but still far apart at 0900. This figure makes it appear that the two auroral equatorward boundaries do not cross on diametrically opposite points, but perhaps only a few hours apart. Perhaps the equatorward boundaries of electron and ion precipitation are not concentric circlesof the same radius, but converge only on the night side of the planet.

The conclusion drawn in that the electron and ion diffuse

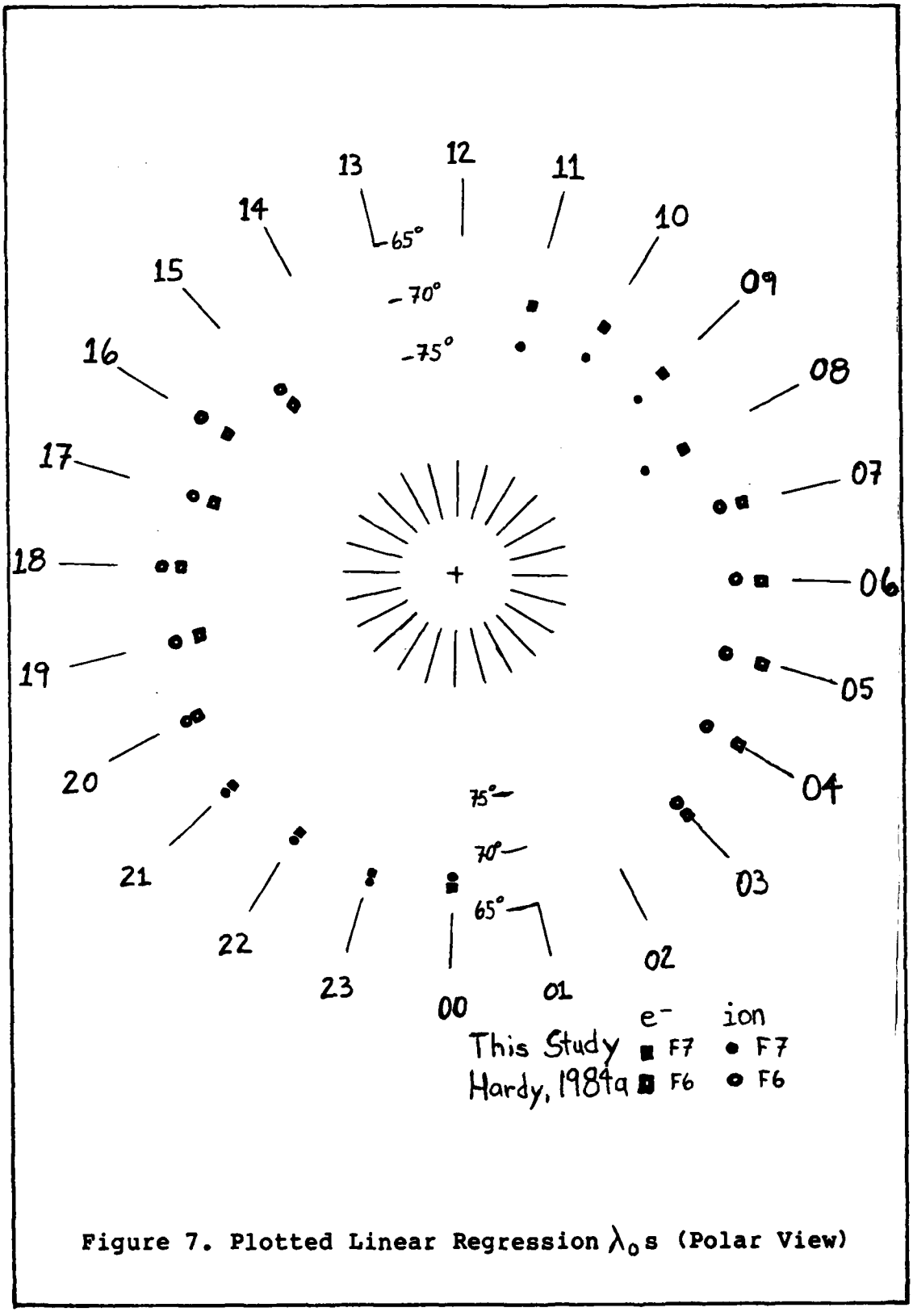

Figure 7. Plotted Linear Regression λ_0s (Polar View)

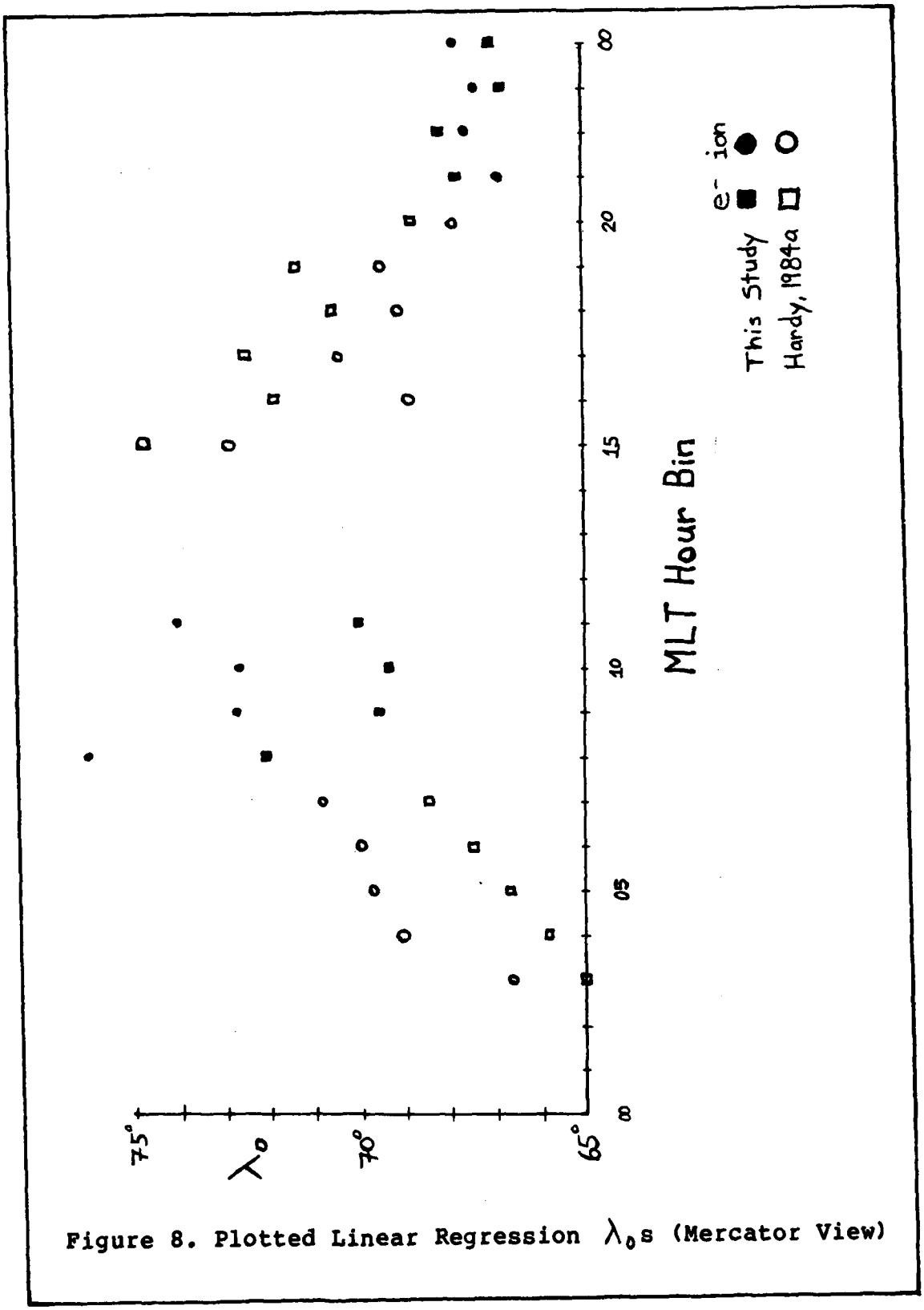

Figure 8. Plotted Linear Regression λ_0s (Mercator View)

auroral equatorward boundaries do cross in the 2100 hour zone. Early predictions that the two auroral equatorward boundaries crossed 12 hours apart do not appear to be correct. Instead, the crossing points appear to be only a few hours apart. This means that the electron and ion auroral ovals are not two concentric circles, but instead, the ion auroral zone is smaller than the electron auroral zone, and is contained almost entirely within the electron auroral zone.

VII Conclusions And Recommendations

Conclusions

The goal of this thesis has been to extend the work of AFGL with auroral particle boundaries with data from a new satellite. This thesis finds similar results to those of the AFGL analyses of DMSP data, and extends the hours of coverage that have been examined.

First, a comparison was done between Kp and ap to check that Kp was the better predictor of the diffuse auroral boundary, when used in linear regression. Research at AFGL has concentrated on the Kp index, and it does indeed appear to be the correct choice. Use of ap could be further investigated using log ap rather than ap.

Previous research has also divided the measured boundaries by hour bins. A comparison between pooling the boundaries in three hour wide bins and pooling in one hour bins concludes that three hour bins do not accurately reflect the behavior of the auroral boundaries.

It also appears that it is acceptable to pool measured boundaries from the North and South poles, and hence pysical symmetry exists between the north and south pole boundaries. This is desireable to maintain higher numbers of boundaries in each hour bin to give statistically better results.

The second part of this effort has been to examine the separation between the electron and ion aurora. This is also following the model of earlier research by AFGL, and extends

their work into new hour bins. Previous research had suggested that the two auroral boundaries would cross in an evening hour bin and then in an hour bin diametrically opposite on the circle. Results here indicate that the difference is zero (the boundaries cross) in the 2100 hour bin, but that the separation 12 hours later is still great. The dayside crossing should be in the 0900 hour bin, assuming fairly circular diffuse auroral equatorward boundaries. The conclusion drawn is that the electron and ion auroral zones are not circles of the same radii, but instead the ion auroral zone is smaller than the electron auroral zone and mostly poleward of it. The ion aurora is poleward on the dayside of the planet, while the electron aurora is poleward on the nightside, and the two crossing points appear to be just a few hour bins apart.

Recommendations

There are still plenty of things to investigate in this field. So far, efforts have concentrated on using the Kp index as the predictor of the response of the auroral boundary. But the Kp index is just another result of the actual driving influence. The response of the auroral oval to changes in the solar wind speed and interplanetary magnetic field strength and direction should be investigated. This might produce a complex relationship - much different from the simple linear relationships used here. Solar wind data and interplanetary magnetic field data require

satellite measurements outside the magnetosphere which are currently difficult to obtain.

Modeling efforts have concentrated on Kp, and it does provide a better linear relationship than does ap. However, AF ap is potentially a better predictor since its values are spaced linearly. The values for Kp are spaced logarithmically. The complete study could be redone, using ap values and a data transformation. The results would probably not change much, however.

AFGL has always subdivided measured auroral equatorward boundaries into hour bins. A better way would be to list each measured boundary with the time of the boundary crossing down to the minute. This would facilitate the study of the precipitation pattern at different longitudes by allowing flexibly sized bins and by allowing longitude (as represented by magnetic local time) to enter the study directly as a continuous second independent variable along with Kp or AF ap.

A similar study could be done to attempt to find the behavior of the polar auroral boundary. This has been attempted with electron data but proved to be difficult. However, the ionic polar precipitation is much cleaner and could provide a good data base.

So far, the minimum auroral boundary latitude has been predicted using a very simple linear equation. This study could be redone with more attention paid to the error terms in an effort to see if a pattern could be discerned. This

could lead to identifying other driving influences on the auroral oval boundary. This study is the one that AFGL was hoping for in this thesis.

Bibliography

Ejiri, Masaki, "Trajectory Traces of Charged Particles in the Magnetosphere", Journal of Geophysical Research, 83:4798 - 4810 (1 October 1978).

Glasstone, Samuel, Sourcebook of the Space Sciences. Princeton, New Jersey: Van Nostrand, 1965.

Gussenhoven, Dr. M. S., et al, 1978 Diffuse Auroral Boundaries and a Derived Auroral Boundary Index. Air Force Geophysics Laboratory, Environmental Research Paper, Number 818. 28 December 1982.

-----. "Systematics of the Equatorward Diffuse Auroral Boundary", Journal of Geophysical Research, 88: 5692 - 5708 (1 July, 1982).

-----. "DMSP/F2 Electron Observations of Equatorward Auroral Boundaries and Their Relationship to Magnetospheric Electric Fields", Journal of Geophysical Research, 86: 768 - 778 (1 February, 1981).

-----. Study of Characteristics of Polar Cap Auroras in DMSP Images. Air Force Office of Scientific Research, Report 79-0012, 29 February, 1980.

Hardy, Dr. D. A., et al, "Precipitating Electron and Ion Detectors (SSJ/4) for the Block 5D/Flight 6 - 10 DMSP Satellites: Calibration and Data Presentation", Air Force Geophysics Laboratory, August 1984. Paper in preparation.

-----. "The Equatorward Boundary of Auroral Ion Precipitation". Air Force Geophysics Laboratory, July 1984. Paper in preparation.

-----. The Precipitating Electron Detectors (SSJ/3) for the Block 5D/Flight 2 - 5 DMSP Satellites: Calibration and Data Presentation. Air Force Geophysics Laboratory, Instrumentation Paper Number 282. 14 September 1979.

Lange, Dr. James J., Maj, USAF, Lecture notes, Physics 4.20, Space Environment. School of Engineering, Air Force Institute of Technology, Wright-Patterson AFB, OH. Summer 1983.

Mullen, Dr. E. G., SCATHA Environmental Atlas. Air Force Geophysics Laboratory Environmental Paper Number 819. 3 January 1983.

Neter, John and William Wasserman, Applied Linear Statistical Models. Homewood, Illinois: Richard D. Irwin, Inc. 1974.

Nie, Norman H., et al, Statistical Package for the Social Sciences (SPSS) (Second Edition). New York: McGraw Hill Book Company, 1975.

Spjeldvik, Walther N. and Paul L. Rothwell, The Earth's Radiation Belts, Air Force Geophysics Laboratory, Environmental Research Paper, Number 854. 20 September 1983.

Vita

Charles D. Phillips was born in Blytheville, Arkansas on 1 November 1956. He graduated from Central High School in San Angelo, Texas in 1974. In April of 1978 he graduated from Angelo State University with a B.S. in Physics and was commisioned in the U.S. Air Force through the ROTC program. After entering active duty, he completed Space Systems training. Subsequently he was assigned to the NORAD Space Computational Center at Cheyenne Mountain, CO, where he served as a crew orbital analyst and as the Assistant Chief Orbital Analyst. From 1982 to 1983 he completed a tour of duty at Clear AFS, Alaska, where he served as a BMEWS crew Senior Director. He entered the Air Force Institute of Technology in May 1983, and completed the Master of Science in Space Operations in December, 1984. His next assignment will be at the Manned Spaceflight Support Group, Johnson Space Center, Houston, TX.

Permanent Address:

121 Stone Ridge Drive

Warner Robins, Ga. 31093

UNCLASSIFIED
SECURITY CLASSIFICATION OF THIS PAGE

AD-A159215

REPORT DOCUMENTATION PAGE

1a. REPORT SECURITY CLASSIFICATION: UNCLASSIFIED	1b. RESTRICTIVE MARKINGS
2a. SECURITY CLASSIFICATION AUTHORITY	3. DISTRIBUTION/AVAILABILITY OF REPORT: Approved for public release, distribution unlimited
2b. DECLASSIFICATION/DOWNGRADING SCHEDULE	
4. PERFORMING ORGANIZATION REPORT NUMBER(S): AFIT/GSO/ENP - ENS/84D-4	5. MONITORING ORGANIZATION REPORT NUMBER(S)
6a. NAME OF PERFORMING ORGANIZATION: School of Engineering; 6b. OFFICE SYMBOL (If applicable): AFIT/ENS	7a. NAME OF MONITORING ORGANIZATION
6c. ADDRESS (City, State and ZIP Code): Air Force Institute of Technology, Wright-Patterson AFB, OH 45433	7b. ADDRESS (City, State and ZIP Code)
8a. NAME OF FUNDING/SPONSORING ORGANIZATION: Space Physics Division; 8b. OFFICE SYMBOL (If applicable): PHP	9. PROCUREMENT INSTRUMENT IDENTIFICATION NUMBER
8c. ADDRESS (City, State and ZIP Code): Air Force Geophysics Laboratory, Hanscom AFB, MA 01731	10. SOURCE OF FUNDING NOS. — PROGRAM ELEMENT NO. / PROJECT NO. / TASK NO. / WORK UNIT NO.
11. TITLE (Include Security Classification): See Box 19	
12. PERSONAL AUTHOR(S): Charles D. Phillips, B.S., Capt, USAF	
13a. TYPE OF REPORT: MS Thesis; 13b. TIME COVERED: FROM _____ TO _____; 14. DATE OF REPORT (Yr., Mo., Day): 1984 December; 15. PAGE COUNT: 70	
16. SUPPLEMENTARY NOTATION	

17. COSATI CODES			18. SUBJECT TERMS (Continue on reverse if necessary and identify by block number)
FIELD	GROUP	SUB. GR.	STATISTICAL ANALYSIS, AURORA, DMSP, POLAR REGIONS, MAGNETOSPHERE
4	1		

19. ABSTRACT (Continue on reverse if necessary and identify by block number)

Title: SYSTEMATICS OF THE AURORAL BOUNDARY AS INDICATED BY PARTICLE PRECIPITATION

Approved for public release: IAW AFR 190-1.
LYNN E. WOLAVER
Dean for Research and Professional Development
Air Force Institute of Technology
Wright-Patterson AFB OH

Thesis Committee: Dr James Lange, Major, USAF
Dr Joseph Coleman, Lt Col, USAF

Abstract: This thesis examined several ways of grouping data acquired by the DMSP/F7 satellite's electron and ion spectrometers, and used that data to decide the relationship between the latitude of the equatorward boundary of the electron and ion diffuse aurora. The statistical analysis was done with the SPSS computer package and data from the Special Sensor J/4 on board the Defense Meteorological Satellite Program F7 (Block 5D)

20. DISTRIBUTION/AVAILABILITY OF ABSTRACT	21. ABSTRACT SECURITY CLASSIFICATION
UNCLASSIFIED/UNLIMITED ☒ SAME AS RPT. ☐ DTIC USERS ☐	UNCLASSIFIED

22a. NAME OF RESPONSIBLE INDIVIDUAL	22b. TELEPHONE NUMBER (Include Area Code)	22c. OFFICE SYMBOL
Dr James Lange, Major, USAF	(513) 255-2012	AFIT/ENP

DD FORM 1473, 83 APR — EDITION OF 1 JAN 73 IS OBSOLETE

SECURITY CLASSIFICATION OF THIS PAGE

spacecraft. The analytic technique used was bivariate linear regression, with the General Linear Test for the equality of two regression lines being used to compare different regression lines.

The analysis of precipitating electrons and ions above the polar regions at about 840 kilometers found that the precipitation at different geomagnetic longitudes can be accurately represented by dividing the measured boundaries according to their magnetic local times of occurrence. Three hour wide bins were attempted, and were found to be less desirable than one hour wide bins. It was found that measured boundaries from the two poles can be combined in a single regression line.

The above results were used to find that the equatorward boundary of the diffuse ion aurora is circular and poleward of the equatorward boundary of the diffuse electron aurora, except for a few hours in the midnight sector. This study finds that one of the points where the ion aurora and electron aurora cross is in the 2100 hour bin.

END

FILMED

11-85

DTIC